PAPER

High conversion efficiency distributed feedback laser from a dye-doped holographic transmission grating

IOP Publishing Journal of Physics D: Applied Physics
J. Phys. D: Appl. Phys. **51** (2018) 045103 (7pp) https://doi.org/10.1088/1361-6463/aa9f6c

High conversion efficiency distributed feedback laser from a dye-doped holographic transmission grating

Lijuan Liu[1], Guiyang Zhang[2,3], Xiaobo Kong[1], Yonggang Liu[2] and Li Xuan[2]

[1] College of Physics and Engineering, Qufu Normal University, Qufu 273165, People's Republic of China
[2] State Key Laboratory of Applied Optics, Changchun Institute of Optics, Fine, Mechanics and Physics, Chinese Academy of Sciences, Changchun 130033, People's Republic of China
[3] University of Chinese Academy of Sciences, Beijing 100049, People's Republic of China

E-mail: llj2007weihai@163.com

Received 11 June 2017, revised 21 September 2017
Accepted for publication 5 December 2017
Published 4 January 2018

Abstract

A high conversion efficiency distributed feedback (DFB) laser from a dye-doped holographic polymer dispersed liquid crystal (HPDLC) transmission grating structure was reported. The alignment polyimide (PI) films were used to control the orientation of the phase separated liquid crystals (LCs) to increase the refractive index difference between the LC and the polymer, so it can provide better light feedback. The lasing wavelength located at 645.8 nm near the maximum of the amplified spontaneous emission (ASE) spectrum with the lowest threshold 0.97 μJ/pulse and the highest conversion efficiency 1.6% was obtained. The laser performance under electric field were also investigated and illustrated. The simple configuration, one-step fabrication organic dye laser shows the potential to realize ultra-low cost plastic lasers.

Keywords: distributed feedback dye laser, holographic polymer dispersed liquid crystal, orientation, high conversion efficiency

(Some figures may appear in colour only in the online journal)

1. Introduction

Organic distributed feedback (DFB) lasers have attracted a lot of interest for their excellent material characteristics and resonator structures [1, 2] since the first report of distributed feedback laser action in a liquid-dye laser [3]. Organic luminescent materials serve as active gain medium with the advantages of broad spectral gain and high luminous efficiency. These merits enable the realization of laser devices with the whole visible spectrum by using a few active materials [4–6]. DFB structures could provide the long gain path and effective wavelength selectivity as coherent Bragg scattering of the coupled waves propagate throughout thousands of the wavelength-scale periodic microstructure [7]. In general, DFB resonator structures can be fabricated by hot embossing [8], electron beam lithography [9], reactive ion etching and interference ablation. These methods are complex and expensive, so new techniques for making the periodic microstructures used in organic lasers need to be developed.

A holographic polymer dispersed liquid crystal (HPDLC) grating structure composed of alternating liquid crystal (LC) and polymer lamellae has drawn much scientific attention due to their potential for various applications including flat-panel displays [10], optical data storage [11] and optical switches for telecommunications [10]. The HPDLC grating provide a periodic refractive index spatial distribution, which can be regarded as a one-dimensional (1D) photonic crystal, thus the HPDLC structure is the natural DFB resonant cavity to realize Bragg selective reflection effect. Moreover, the holographic method to manufacture HPDLC structure has the advantages of one-step process, low cost, easy to vary the period and pollution-free [12, 13]. When lasing dye is doped in this DFB structure, a micro-miniature organic dye

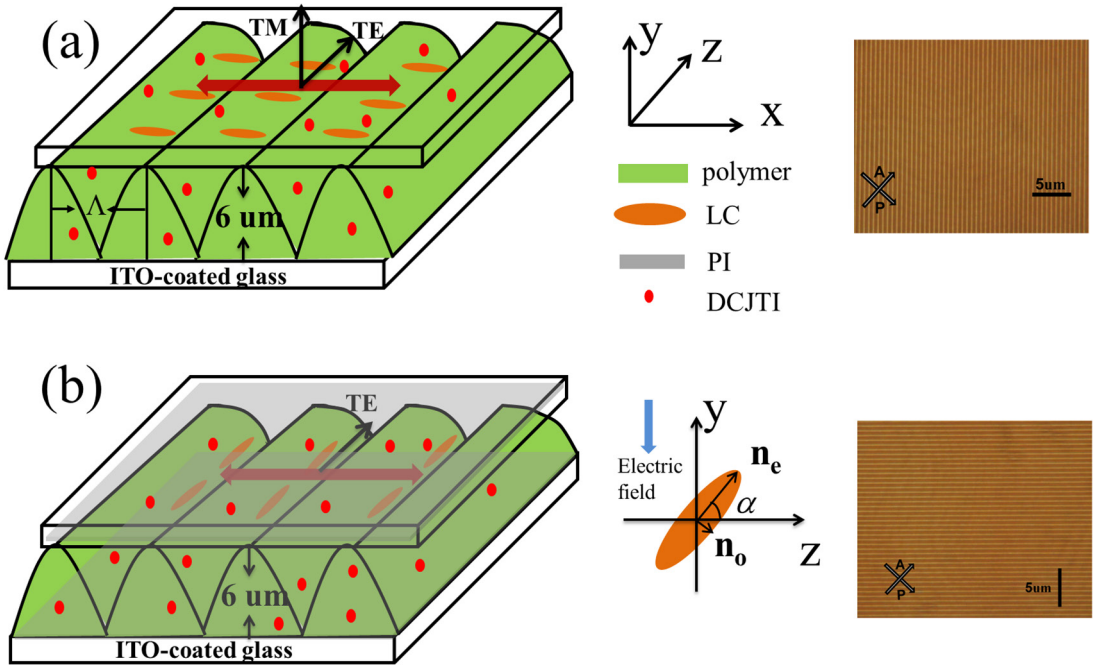

Figure 1. Device structures of (a) without the PI alignment layer and (b) with the PI alignment layer. The insets show the 3D coordinates, tilt angle α of LC molecules under an electric field and POM images of corresponding gratings (polarizer and analyzer axes are oriented in the image).

laser was formed and it can be pumped by Nd:YAG laser or laser diodes which show the potential to be integrated in all optical devices [5]. Furthermore, the lasing wavelength from dye-doped HPDLC can be controlled precisely by a thermal or electrical method due to the large optical and dielectric anisotropies of LCs [14, 15]. Undoubtedly, this packaged multifunctional dye-doped organic laser will be widely used in the future.

In this paper, we present an organic DFB dye laser based on the HPDLC transmission grating structure. The laser dye doped here was 2-[2-(1-Methylethyl)-6-[2-(2, 3, 6, 7-tetrahydro-1, 1, 7, 7-tetramethyl-1H, 5H-benzo [*ij*] quinolizin-9-yl) ethenyl]-4 H-pyran-4-ylidene] propanedinitrile (DCJTI), which was homogeneous dispersed in the HPDLC grating layer. Therefore, only refractive index spatial modulation exists in the structure and gain modulation can be neglected. Different from previous reports [14–17], only a low functional monomer was used and the rubbed PI layer was spin-coated on the substrate to control the orientation of the phase separated LCs along the groove direction of HPDLC grating. In this way, the refractive index of the phase separated LCs changed from ordinary refractive index (n_o) to extraordinary refractive index (n_e) for TE polarized light and the refractive index difference between LC and polymer lamellae was increased, thus the light feedback was improved.

2. Experiments

2.1. Device structure and materials

The device structure is illustrated in figure 1. The core layer of the proposed laser device is made from HPDLC grating doped with laser dye DCJTI. While the top glass substrate and bottom glass substrate are used as cladding layers to form glass substrate/HPDLC-grating/glass substrate configuration as a symmetric slab waveguide. we applied PI (Merck) as an alignment layer to control LC alignment in some samples, as illustrated in figure 1(b). The PI film was spin-coated onto the surface of the cleaned ITO coated glass substrate and baked at 250 °C for 2 h, and followed by unidirectional rubbed to control LC alignment along the groove direction of HPDLC grating (z axis). The prepolymer syrup for fabricating HPDLC grating consists of 57.5 wt% difunctional acrylate monomer phthalic diglycol diacrylate (PDDA, Sigma-Aldrich), 30 wt% nematic LC, E7, ($n_o = 1.521$, $n_e = 1.746$, Merck), 10 wt% N-vinylpyrrolidone (NVP, Sigma-Aldrich), 0.5 wt% photo-initiator Rose Bengal (RB, Sigma-Aldrich), 1.5 wt% coinitiator N-phenylglycine (NPG, Sigma-Aldrich) and 0.5 wt% DCJTI. It was stirred for 12 h in the dark until we obtained a homogeneous mixture. Then the mixture was injected into empty cell by capillary action at room temperature. The cell gap was controlled at 6 μm by Mylar spacers.

2.2. Absorption and photoluminescence (PL) spectrum measurement

For absorption and PL measurement, the cell with homogeneous prepolymer syrup was irradiated under a single laser beam from a Nd:YAG laser (532 nm, 10 mW cm^{-2}) for 10 min. This homogenous illumination would result in the homogenous dispersion of LC droplets in the polymer matrix which is referred to as polymer dispersed liquid crystal (PDLC). The absorption and photoluminescence (PL) spectrum of DCJTI-doped HPDLC film were measured by a UV–vis spectrophotometer (Shimadzu UV-3101; Shimadzu Corp., Kyoto, Japan)

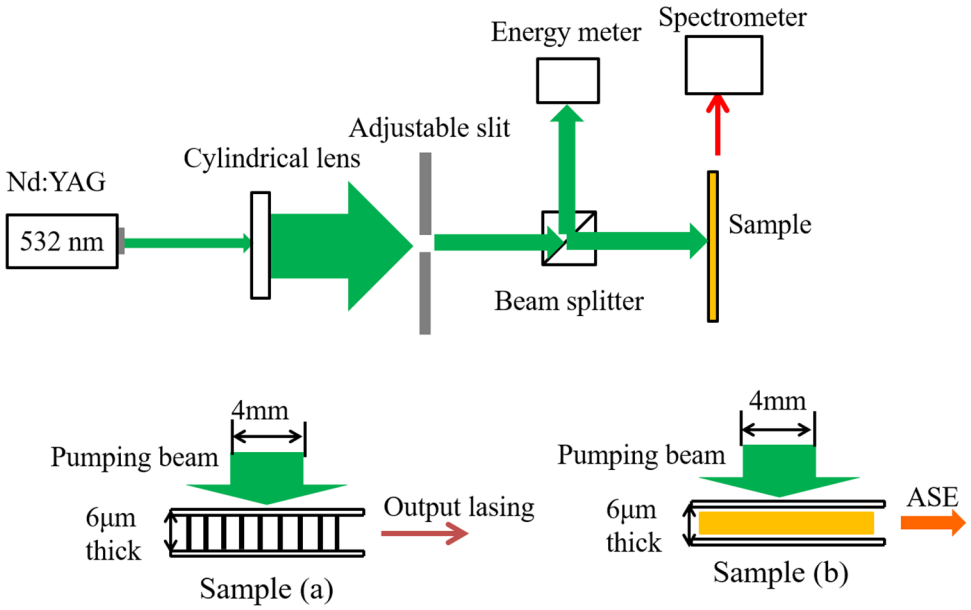

Figure 2. Schematic set-up for the lasing (a) and ASE (b) measurement.

and fluorescence spectrophotometer (Hitachi F-7000; Hitachi, Ltd., Tokyo, Japan), respectively.

2.3. HPDLC grating fabrication

Two types of cells with homogeneous prepolymer syrup were exposed to the interference patterns generated by two coherent *s*-polarized laser beams from a 532 nm Nd:YAG laser, respectively [18, 19]. The light intensity of each recording beam was 2.5 mW cm^{-2} and the exposure time was 3 min. The cured grating area was 8 mm by 8 mm. The HPDLC grating period (Λ) can be controlled according to

$$\Lambda = \frac{\lambda_{532}}{2\sin(\theta/2)} \quad (1)$$

by changing the intersection angle (θ) between the two coherent lasing beams.

2.4. Lasing measurement

The lasing and the amplified spontaneous emission (ASE) property of the device was investigated under ambient atmosphere using a frequency-doubled, pulsed Nd-YAG laser (532 nm, 8.6 ns, 2 Hz). The schematic setup is shown in figure 2. The pumping beam was divided by a beam splitter into two beams with equal intensity. The energy of one beam was detected by an energy meter directly, and the other beam was shaped by a cylindrical lens with focal length 20 cm into a strip. The width of the strip was about 0.1 mm, and the length of the strip was 4 mm controlled by an adjustable slit. Sample (a) in figure 2 is a HPDLC grating for lasing measurement. The focused stripe can cover thousands of grating periods, and thus ensures sufficient DFB. Sample (b) without grating structure is a PDLC sample for ASE measurement. The reason is that ASE does not require a resonator structure, but a sufficient number of excited states along the optical path [20]. The emitted light was collected from the edge of the sample with an optical fiber spectrometer and the energy meter was used to measure the output laser energy.

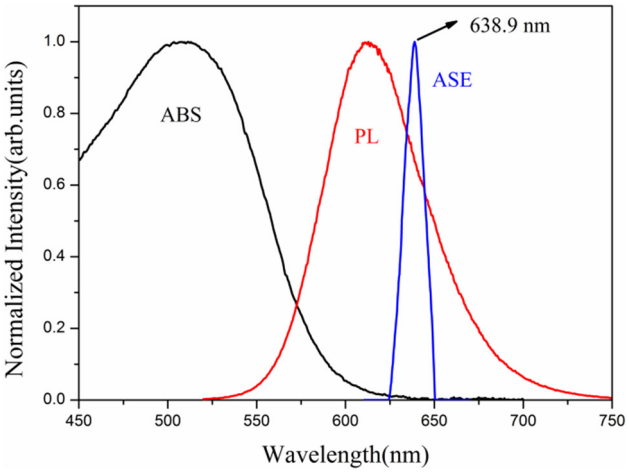

Figure 3. Absorption, PL and ASE spectrum of DCJTI-doped polymer HPDLC film.

3. Results and discussion

3.1. The absorption, PL and ASE spectrum of DCJTI-doped polymer HPDLC film

In order to evaluate the scope of organic dye laser, the absorption and PL spectrum of DCJTI were measured and shown in figure 3. The broad absorption spectrum shown here range from 450 nm to 625 nm and the PL spectrum extend from 525 nm to 750 nm. The obvious overlap between the absorption band and the PL band from 525 nm to 600 nm meaning that laser action cannot be obtained well in this spectral range because of the reabsorption effect. Furthermore, ASE spectrum, which can be regard as a signal of the lasing performance of the gain medium [20, 21], was measured and the

Table 1. Parameters of different samples in the experiment.

Period (nm)	η_p (%)	η_s(%)	η_p/η_s	η_p^* (%)	η_s^*(%)	η_p^*/η_s^*
596	82.3	2.7	30.5	3.5	79.8	1/22.8
605	85.8	2.8	30.6	3.7	78.9	1/21.3
617	88.2	1.9	46.4	2.8	85.3	1/30.5
628	76.3	2.3	33.2	2.7	75.6	1/28.1
637	83.7	1.8	46.5	2.1	76.5	1/36.4
646	87.4	2.2	39.7	2.5	81.3	1/32.5

Note: η_p and η_s were the diffraction efficiency of p and s polarization states for samples without rubbed PI films, η_p^* and η_s^* were the diffraction efficiency of p and s polarization states for samples with rubbed PI films.

peak located at 638.9 nm with a full width at half maximum (FWHM) of nearly 10 nm. These results told us the organic dye laser must be well-designed and the output lasing should be near the ASE peak.

3.2. Diffraction efficiency for HPDLC gratings

To determine the orientation of LC molecules, the diffraction efficiency of each sample was measured. The diffraction efficiency is defined as the first order diffracted light intensity (I_{1_χ}) plus the zeroth order light intensity (I_0) and then divided by I_{1_χ}, here χ is the s or p polarization state obtained by rotating the polarizer in the light path. The parameters of each sample are shown in table 1.

The p light diffraction efficiency (η_p) is greater than the s light diffraction efficiency (η_s) for samples without rubbed PI films, and the grating optical sensitivity η_p/η_s is greater than 30. However, η_s for samples with rubbed PI films is larger than η_p and the η_p/η_s is smaller than 1/20. When a He–Ne laser incident onto the sample at the Bragg angle, the s polarization state is parallel to z axis and p polarization state is parallel to x axis. As shown in figure 1(a), LCs align along x axis due to the formation of polymer filaments across the polymer walls during the fabricating process [17]. Therefore, the p-polarized light experiences the extraordinary refractive index (n_e) and s-polarized light share the ordinary refractive index (n_o) of the LCs. Considering that the refractive index of polymer (1.529) is close to n_o of the LCs, the higher diffraction efficiency of p polarized light and the lower diffraction efficiency of s polarized light were obtained. When PI films were applied, as shown in figure 1(b), the LCs arrange along z axis. Thus, the s-polarized light has the extraordinary refractive index (n_e) and p-polarized light share the ordinary refractive index (n_o) of the LCs and the opposite diffraction efficiency values for samples with rubbed PI were achieved.

3.3. Laser performance

DFB lasing relies on the positive feedback distributed in the periodic structure. The condition for feedback is given by the Laue condition [22]:

$$2\vec{k}\cdot\vec{G} = \left|\vec{G}\right|^2 \tag{2}$$

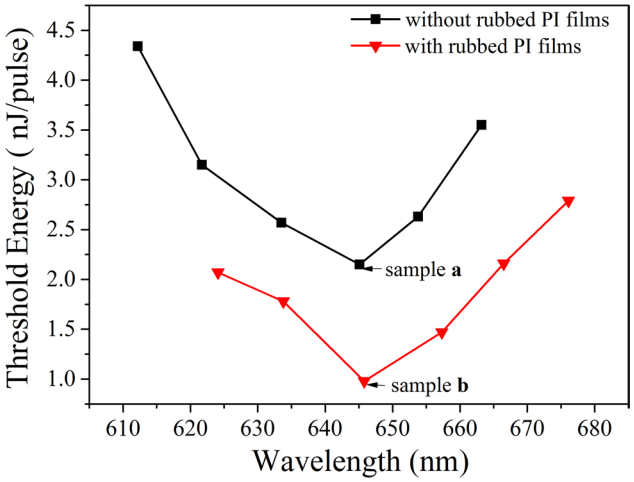

Figure 4. Dependence of threshold energy on the lasing wavelength for samples without rubbed PI films (sphere) and samples with rubbed PI films (bottom triangle), respectively.

where the wave-vector of the guided mode is $k = n_{\text{eff}}k_0$ (n_{eff} is the effective index of the guided mode and k_0 is the free-space vector number) and G denotes of the reciprocal lattice of the periodic dielectric structure with $G = m\cdot 2\pi\Lambda^{-1}$ (where m iselected as 3 in this work and Λ is the grating period). Substituting k and G to equation (2), it can be expressed as:

$$2\left(n_{\text{eff}}\frac{2\pi}{\lambda}\right)\left(m\frac{2\pi}{\Lambda}\right) = \left(m\frac{2\pi}{\Lambda}\right)\left(m\frac{2\pi}{\Lambda}\right). \tag{3}$$

After simplification, the lasing wavelength λ can be finally expressed as:

$$\lambda = \frac{2n_{\text{eff}}\Lambda}{m}. \tag{4}$$

The lasing threshold as a function of output wavelength is shown in figure 4. Although the grating periods of two types of samples were same, as listed in table 1, their lasing performance was different. Lower threshold was measured for samples with rubbed PI films. The lowest threshold obtained for samples without rubbed PI films called sample **a** ($\Lambda = 628$ nm, $\eta_p = 76.3\%$, $\eta_s = 2.3\%$, as listed in table 1) and the lowest threshold obtained for samples with rubbed PI films called sample **b** ($\Lambda = 617$ nm, $\eta_p = 2.8\%$, $\eta_s = 85.3\%$, as listed in table 1). Sample **a** and sample **b** are marked in figure 4 by arrows. The dependence of output energy on the input energy for sample **a** and sample **b** were shown in figure 5. The lasing output was obtained by the intersection of the linear fitting curve. The threshold is 2.21 μJ/pulse for sample **a** and the conversion efficiency of pump input to the lasing output is 0.7%. However, the lasing output properties of sample **b** is greatly improved, as shown in figure 5(b). The threshold was decreased to 0.97 μJ/pulse and the conversion efficiency was increased to 1.6%. The lasers emitted from sample **a** and sample **b** located at 645.1 nm and 645.8 nm with the FWHM of 0.5 nm and 0.4 nm, respectively. To date, there are only two reports on the conversion efficiency for the laser from dye-doped HPDLCs, which are around 0.1% and 0.8% [15, 23].

We attributed the improvement of conversion efficiency to several aspects. First of all, the HPDLC structure serves as

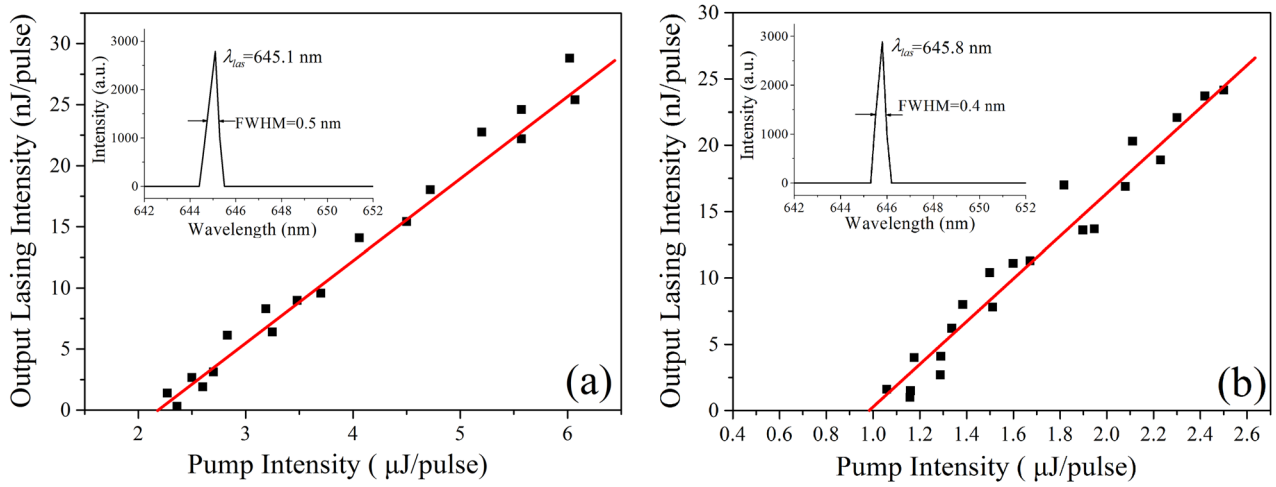

Figure 5. Lasing output intensity as a function of pump intensity for the DFB laser: (a) sample **a**, (b) sample **b**. The insets show the corresponding lasing spectra, respectively.

laser resonator was fabricated with low-functional monomer (PDDA) and under low curing intensity (2.5 mW cm^{-2} per recording beam), the low curing intensity would lead to form polymer scaffolding morphology holographic grating [17, 24]. There were no LC droplets in the LCs-rich lamellae, thus the scattering loss was lower (<6%) [2] than droplet-like morphology holographic grating [16, 25] whose LC droplets size are comparable to visible wavelengths. Meanwhile, the low curing intensity would not lead to the photodegradation of the lasing dye during the fabricating process which ensures the laser emission. Furthermore, the refractive index modulation Δn between the LCs-rich and polymer-rich lamellae was greatly increased by controlling the orientation of LCs. The refractive index modulation Δn can be calculated according to the isotropic coupled wave theory [26]:

$$\Delta n = \frac{\lambda_{633} \arcsin \sqrt{\eta_s} \cos \theta_B}{\pi d} \quad (5)$$

where λ_{633} is the wavelength of He–Ne laser, η_s is the diffraction efficiency of *s*-polarized light, θ_B is the Bragg angle and d is the cell thickness. Considering the parameters shown in table 1, the refractive index modulation Δn was increased from 0.0039 for sample **a** to a relatively high value of 0.041 for sample **b**. The higher the Δn, the larger the coupling coefficient, and it will reduce the threshold and the slope efficiency. However, the bigger the Δn in the grating vector direction (the lasing feedback direction), the better the lasing feedback performance, and it will increase the slope efficiency. The impact of the better lasing feedback is stronger than the larger coupling coefficient on slope efficiency, therefore we have a lower threshold and a higher slope efficiency at last.

The lasing modes from sample **a** and sample **b** have been studied and both transverse magnetic (TM) and transverse electric (TE) modes exist in the HPDLC structure [16]. As shown in figure 1(a), the laser propagates along the grating vector direction (*x* axis), TM and TE modes share the same ordinary refractive index (n_o) with the same refractive index modulation Δn value 0.0039. While in figure 1(b), LCs align along the groove direction (*z* axis) of HPDLC grating, thus

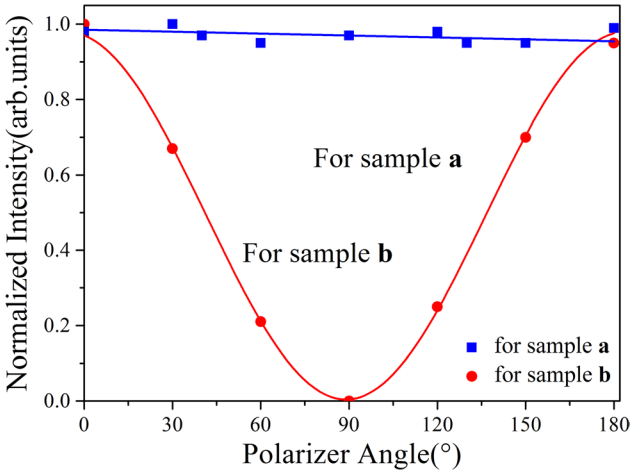

Figure 6. The transmitted intensity of lasers from sample **a** and sample **b** on the dependence of the rotation angle.

TM mode occupies the ordinary refractive index (n_o) with the refractive index modulation Δn value 0.0039, which is the same with sample **a**. However, TE mode enjoys the extraordinary refractive index (n_e) with the larger refractive index modulation Δn value 0.041. Thus TE mode has better light feedback and TM mode is disappeared. That is to say, the laser from sample **b** only contains TE mode.

For measuring lasing polarization state, a polarizer was set between the sample and the optical fiber spectrometer. The transmitted light polarization direction was varied with the rotation angle and TE mode corresponds to 0°. Figure 6 illustrated the transmitted intensity of lasers on the dependence of the rotation angle. The results of the experiments also showed that the output laser from sample **a** contained TE and TM modes, while that from sample **b** only contained TE mode.

As the organic dye laser was formed based on LCs-doped HPDLC feedback structure, we can anticipate that the emitted laser can be controlled by changing the refractive index modulation of HPDLC grating due to the rotation of LCs in *z*-*y* plane under an electric field. The emitted lasing wavelength and corresponding lasing intensity as a function of the applied

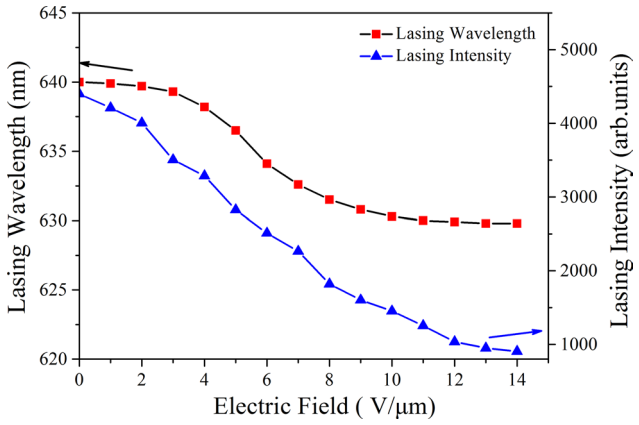

Figure 7. The relationship between the lasing wavelength, lasing intensity and electric field for sample **b**.

electric field for sample **b** were illustrated in figure 7. The laser wavelength blue shift from 640 to 629.8 (nm) and the corresponding lasing intensity decreased from 4400 to 900 (arb. units) with the electric field increased to 14 $\mathrm{V}\,\mu\mathrm{m}^{-1}$. These results were attributed to the decrease of the refractive index modulation of HPDLC grating under electric field, which also implied the bigger refractive index modulation the higher conversion efficiency.

4. Conclusion

In this paper, we studied the effects of the alignment PI film on lasing output threshold and conversion efficiency based on glass substrate/HPDLC-grating/glass laser configuration. The results indicate that the alignment PI film on the substrate can make LC molecules align along the designed rubbing direction. The refractive index modulation was increased from 0.0039 to a relatively high value of 0.041 and lasing performance was greatly improved. The polarization of emitted lasing output beams and electrical control of the DFB laser were also investigated. The research will widen the applications of organic DFB laser in the field of laser displays and integrated photonic circuits.

Acknowledgments

The authors would like to thank the National Natural Science Foundation of China (grant numbers (61475152), (61377032) and (61405194)) for their support.

ORCID iDs

Lijuan Liu https://orcid.org/0000-0003-0401-8470

References

[1] Huang W, Diao Z, Yao L, Cao Z, Liu Y, Ma J and Xuan L 2013 Electrically tunable distributed feedback laser emission from scaffolding morphologic holographic polymer dispersed liquid crystal grating *Appl. Phys. Express* **6** 022702

[2] Liu L, Xuan L, Zhang G, Liu M, Hu L, Liu Y and Ma J 2015 Enhancement of pump efficiency for an organic distributed feedback laser based on a holographic polymer dispersed liquid crystal as an external light feedback layer *J. Mater. Chem.* C **3** 5566–72

[3] Shank C, Bjorkholm J and Kogelnik H 1971 Tunable distributed-feedback dye laser *Appl. Phys. Lett.* **18** 395–6

[4] Klinkhammer S, Liu X, Huska K, Shen Y, Vanderheiden S, Valouch S, Vannahme C, Bräse S, Mappes T and Lemmer U 2012 Continuously tunable solution-processed organic semiconductor DFB lasers pumped by laser diode *Opt. Express* **20** 6357–64

[5] Samuel I and Turnbull G 2007 Organic semiconductor lasers *Chem. Rev.* **107** 1272–95

[6] Xiang C, Koo W, So F, Sasabe H and Kido J 2013 A systematic study on efficiency enhancements in phosphorescent green, red and blue microcavity organic light emitting devices *Light: Sci. Appl.* **2** e74

[7] Smirnova T, Sakhno O, Stumpe J, Kzianzou V and Schrader S 2011 Distributed feedback lasing in dye-doped nanocomposite holographic transmission gratings *J. Opt.* **13** 035709

[8] Wenger B, Tétreault N, Welland M E and Friend R H 2010 Mechanically tunable conjugated polymer distributed feedback lasers *Appl. Phys. Lett.* **97** 193303

[9] Xia R, Heliotis G, Stavrinou P and Bradley D 2005 Polyfluorene distributed feedback lasers operating in the green-yellow spectral region *Appl. Phys. Lett.* **87** 031104

[10] Li M S, Wu S T and Fuh A Y-G 2006 Superprism phenomenon based on holographic polymer dispersed liquid crystal films *Appl. Phys. Lett.* **88** 091109

[11] Simoni F, Cipparrone G, Mazzulla A and Pagliusi P 1999 Polymer dispersed liquid crystals: effects of photorefractivity and local heating on holographic recording *Chem. Phys.* **245** 429–36

[12] Huang W, Liu Y, Hu L, Mu Q, Peng Z, Yang C and Xuan L 2013 Second-order distributed feedback polymer laser based on holographic polymer dispersed liquid crystal grating *Org. Electron.* **14** 2299–305

[13] Diao Z, Deng S, Huang W, Xuan L, Hu L, Liu Y and Ma J 2012 Organic dual-wavelength distributed feedback laser empowered by dye-doped holography *J. Mater. Chem.* **22** 23331–4

[14] Liu L, Huang W, Diao Z, Peng Z, Mu Q Q, Liu Y, Yang C, Hu L and Xuan L 2014 Low threshold of distributed feedback lasers based on scaffolding morphologic holographic polymer dispersed liquid crystal gratings: reduced losses through Forster transfer *Liq. Cryst.* **41** 145–52

[15] Huang W, Liu Q, Xuan L and Chen L 2014 Single-mode lasing from dye-doped holographic polymer-dispersed liquid crystal transmission gratings *Appl. Phys.* B **117** 1065–71

[16] Liu Y, Sun X, Shum P, Li H, Mi J, Ji W and Zhang X 2006 Low-threshold and narrow-linewidth lasing from dye-doped holographic polymer-dispersed liquid crystal transmission gratings *Appl. Phys. Lett.* **88** 061107

[17] Huang W, Liu Y, Diao Z, Yang C, Yao L, Ma J and Xuan L 2012 Theory and characteristics of holographic polymer dispersed liquid crystal transmission grating with scaffolding morphology *Appl. Opt.* **51** 4013–20

[18] Bunning T, Natarajan L, Tondiglia V and Sutherland R 2000 Holographic polymer-dispersed liquid crystals (H-PDLCs) *Annu. Rev. Mater. Sci.* **30** 83–115

[19] Hsiao V K, Yong K-T, Cartwright A N, Swihart M T, Prasad P N, Lloyd P F and Bunning T J 2009 Nanoporous polymeric photonic crystals by emulsion holography *J. Mater. Chem.* **19** 3998–4003

[20] Kretsch K P, Belton C, Lipson S, Blau W J and Henari F Z 1999 Amplified spontaneous emission and optical gain spectra from stilbenoid and phenylene vinylene derivative model compounds *J. Appl. Phys.* **86** 6155–9
[21] Tsutsumi N, Kawahira T and Sakai W 2003 Amplified spontaneousemission and distributed feedback lasing from a conjugated compound in various polymer matrices *Appl. Phys. Lett.* **83** 2533–5
[22] Riechel S, Lemmer U, Feldmann J, Benstem T, Kowalsky W, Scherf U, Gombert A and Wittwer V 2000 Laser modes in organic solid-state distributed feedback lasers *Appl. Phys.* B **71** 897–900
[23] Hsiao V K S, Lu C, He G S, Pan M, Cartwright A N and Prasad P N 2005 High contrast switching of distributed-feedback lasing in dye-doped H-PDLC transmission grating structures *Opt. Express* **13** 3787–94
[24] Vardanyan K, Qi J, Eakin J, De Sarkar M and Crawford G 2002 Polymer scaffolding model for holographic polymer-dispersed liquid crystals *Appl. Phys. Lett.* **81** 4736–8
[25] Sutherland R, Tondiglia V, Natarajan L, Lloyd P and Bunning T 2006 Coherent diffraction and random scattering in thiol-ene–based holographic polymer-dispersed liquid crystal reflection gratings *J. Appl. Phys.* **99** 123104
[26] Kogelnik H 1969 Coupled wave theory for thick hologram gratings *Bell Syst. Tech. J.* **48** 2909–47